

Received: 2020.11.25
Accepted: 2021.02.27
Available online: 2021.03.19
Published: 2021.06.14

Helenalin Facilitates Reactive Oxygen Species-Mediated Apoptosis and Cell Cycle Arrest by Targeting Thioredoxin Reductase-1 in Human Prostate Cancer Cells

Authors' Contribution:

Study Design A
Data Collection B
Statistical Analysis C
Data Interpretation D
Manuscript Preparation E
Literature Search F
Funds Collection G

A 1 **Mei Yang**
B 2 **Weihua Zhang**
C 3 **Xiuxiu Yu**
D 3 **Feng Wang**
E 3 **Yeping Li**
F 3 **Yan Zhang**
AG 3 **Yu Yang**

1 Department of Intensive Care Unit, The First Affiliated Hospital of Wenzhou Medical University, Wenzhou, Zhejiang, P.R. China
2 Department of Internal Medicine, Traditional Chinese Medical Hospital of Huzhou, Huzhou, Zhejiang, P.R. China
3 Department of Urology, The First Affiliated Hospital of Wenzhou Medical University, Wenzhou, Zhejiang, P.R. China

Corresponding Author: Yu Yang, e-mail: yangu@wmu.edu.cn

Source of support: This work was funded by Wenzhou Science and Technology Plan Fund Self-Raised Project (Y20180481), Zhejiang Provincial Natural Science Foundation of China (LY21H050006)

Background: Helenalin is a pseudoguaianolide natural product with anti-cancer activities. This study investigated the underlying mechanism of the anti-prostate cancer effects of helenalin in vitro.

Material/Methods: CCK-8 assay was performed to detect the optimal concentrations of helenalin in DU145 and PC-3 cells. After exposure to helenalin and/or reactive oxygen species (ROS) inhibitor, ROS production was assessed by DCFH-DA staining. Thioredoxin reductase-1 (TrxR1) expression was detected by RT-qPCR and western blot. Moreover, apoptosis and cell cycle were evaluated by flow cytometry. Following TrxR1 knockdown or overexpression, TrxR1 expression, ROS generation, apoptosis, cell cycle, migration, and invasion were examined in cells co-treated with helenalin.


Results: Helenalin distinctly repressed the viability of prostate cancer cells in a concentration-dependent manner. We chose 8 μ M and 4 μ M as the optimal concentrations of helenalin for DU145 and PC-3 cells, respectively. Helenalin treatment markedly triggered ROS production and lowered TrxR1 expression, which was ameliorated by ROS inhibitor. Exposure to helenalin facilitated apoptosis as well as G0/G1 cell cycle arrest, which was reversed by ROS inhibitor. Helenalin relieved the inhibitory effect of TrxR1 on ROS production. Furthermore, helenalin ameliorated the decrease in apoptosis rate and the shortening of G0/G1 phase as well as the increase in migration and invasion induced by TrxR1 overexpression.

Conclusions: Our findings revealed that helenalin accelerated ROS-mediated apoptosis and cell cycle arrest via targeting TrxR1 in human prostate cancer cells.

Keywords: **Apoptosis • Cell Cycle • Prostatic Neoplasms • Reactive Oxygen Species • Thioredoxins**

Abbreviations: **ROS** – reactive oxygen species; **TrxR1** – thioredoxin reductase-1; **Trx** – thioredoxin; **CCK-8** – Cell Counting Kit-8; **OD** – optical density; **ER** – endoplasmic reticulum; **RT-qPCR** – real-time quantitative PCR

Full-text PDF: <https://www.medscimonit.com/abstract/index/idArt/930083>

 3660

 —

 7

 36



Background

Prostate cancer is one of the leading malignancies among men globally, with considerably high morbidity and mortality [1]. Its progression is associated with apoptosis, proliferation, and metastasis [2]. Androgen deprivation is the standard therapeutic strategy [3]. Nevertheless, prostate cancer cells become insensitive to anti-androgen treatment, which limits treatment options [4]. Therefore, there is an urgent need to develop or identify novel drugs for treating this deadly disease.

Oxidative stress is involved in regulation of malignant biological behavior of tumor cells [5]. Although a certain level of ROS is needed for maintenance of cell function in terms of normal physiology, excessive ROS can disrupt the pro-oxidant and antioxidant balance, thereby inducing cell damage or death [6]. It has been established that there is more oxidative stress in cancer cells than in normal cells [7]. Increase in the level of oxidative stress could become a promising treatment strategy to eliminate tumor cells [8]. For prostate carcinoma cells, there is a gain in ROS generation as well as oxidative stress [9]. Hence, inducing the production of ROS can kill prostate cancer cells [10]. The thioredoxin (Trx) system can mediate the redox balance in various cells, containing TrxR, Trx, and NADPH [11]. Trx, as an intermediate, can sense the cellular redox state and transmit information to signaling molecules. It has been reported that Trx1 regulates apoptosis of prostate cancer cells induced by bioactive compounds [12]. Furthermore, Trx1 protects against androgen receptor-mediated redox vulnerability in castration-resistant prostate cancer [13]. Thus, Trx1 may act as a subcellular marker of redox imbalance in prostate cancer development [14]. TrxR can degrade Trx; therefore, suppression of its activity destroys the redox balance of cells, thereby leading to an increase in ROS levels [15]. TrxR has been found to be overexpressed in prostate cancer and is correlated with drug resistance [16]. These studies highlight the key roles of the Trx system in the progression of prostate cancer.

Helenalin is a pseudoguaianolide natural product with numerous pharmacological activities against inflammation [17], oxidative stress [18], and cancers [19]. A series of cellular experiments have shown that helenalin is toxic to tumor cells, but not to normal cells, indicating that helenalin may be effective as a low-level toxicant for prostate cancer [20]. Although the anti-cancer activity of helenalin has been reported in various cancers [17,21,22], whether helenalin can limit prostate cancer progression remains unclear, and the underlying mechanisms behind these effects have not been completely clarified. Here, we investigated the promotion effects of helenalin on ROS-dependent apoptosis as well as cell cycle arrest via TrxR1 in 2 prostate carcinoma cell lines. Our study results offer theoretical and experimental evidence for developing candidate novel drugs for prostate cancer.

Material and Methods

Cell Culture

Normal prostate RWPE1 cells, human prostate cancer DU145 and PC-3 cells, and human neuroendocrine prostate cancer NCI-H660 cells were purchased from the American Type Culture Collection (ATCC; USA). RWPE1 cells were cultured in K-SFM basal medium containing keratinocyte-SFM growth supplement (10744-019; Gibco, Grand Island, New York, USA) and BPE. DU145 and NCI-H660 cells were cultured in RPMI-1640 medium (PM150410; Procell, Wuhan, China) plus 10% fetal bovine serum (FBS; SH30084.03; Hyclone, Logan City, Utah, USA), while PC-3 cells were grown in F-12K (21127-022; Gibco) medium+10% FBS (C10010500BT; Life, USA). The culture medium contained 100 U/mL penicillin and 100 U/mL streptomycin. These cells were grown at 37°C and 5% CO₂ with saturated humidity. Cells in logarithmic growth phase were used for further experiments.

Cell Counting Kit-8 (CCK-8)

CCK-8 assay was performed to determine the cell viability via a CCK-8 detection kit (CK04; Dojindo, Shanghai, China). After washing with PBS (C10010500BT; Life Carlsbad, California, USA), RWPE1, DU145, PC-3, and NCI-H660 cells were trypsinized for 2 min, and then pipetted into single cells. We added 20 µl cell suspension to 20 µl trypan blue for cell counting. The remaining cell suspension was centrifuged at 1000 rpm for 5 min. After resuspension in the corresponding medium, cells were plated into 96-well plates (8000 cells/well). After being cultured to adhere to the wall, the cells were added with different concentrations of helenalin (0, 0.5, 1, 2, 4, 8, 12, 16, 20 µM) and cultured for 48 h. Then, cells were incubated with CCK-8 solution for 3 h. After adding the stop solution, the optical density values (OD) were determined at 490 nm utilizing a fully functional microporous plate detector (envision; PerkinElmer, Shanghai).

Transfection

To silence TrxR1 expression, DU145 and PC-3 cells were inoculated onto a 6-well plate (1×10⁴ cells/well). After culture for 24 h, 50 pmol/mL siRNAs targeting TrxR1 (GenePharma, Shanghai, China) or controls were transfected into cells by lipofectamine 2000 reagent (Invitrogen, USA). The sequences of siRNAs were as follows: si-TrxR1#1: GGGTAAGACCCTGGTTGTT; Si-TrxR1#2: CCACTGTATTACTCCTTT; si-TrxR1#3: GCAGCTGGACAGACAATT. To overexpress TrxR1, the recombinant plasmid vector coding TrxR1 protein (GenePharma) was transfected into DU145 and PC-3 cells via lipofectamine 2000 (Invitrogen). After 24 h, the transfection effects were assessed by real-time quantitative PCR (RT-qPCR) and western blot.

Immunofluorescence

A reactive oxygen detection kit (CA1410; Solarbio, Beijing, China) was utilized to detect ROS in DU145 or PC-3 cells. Cover slips were placed in a 24-well plate (1 piece/well). Cells were inoculated into each well (1×10^4 cells/well). After the cells adhered, they were pre-treated with N-acetyl cysteine (NAC), an ROS inhibitor, for 1 h, followed by treatment with helenalin. After 48 h, 2',7'-dichlorofluorescein diacetate (DCFH-DA) was diluted to 1: 1000 by serum-free medium to make the final concentration $10 \mu\text{mol/L}$. The cells were incubated with $300 \mu\text{l}$ DCFH-DA at 37°C for 30 min. After PBS immersion, 4% paraformaldehyde (E672002; Sangon Biotech, Shanghai, China) was used to fix the climbing sections (801007; NEST, Wuxi, China) for 15 min. Then, the slides were permeated by 0.5% Triton X-100 (T8787; Sigma, USA) for 20 min at room temperature. After immersion, normal goat serum (C0265; Beyotime, Beijing, China) was added dropwise to the sections and blocked at room temperature for 30 min. DAPI (D9542; Sigma) was dropped on the sections and incubated in the dark for 5 min. The slides were mounted with mounting solution containing anti-fluorescence quencher. The images were observed under a fluorescence microscope (BX53; Olympus, Japan).

RT-qPCR

RNA was extracted from DU145 or PC-3 cells using the MiniBEST Universal RNA Extraction Kit (9767; TaKaRa, Beijing, China). The OD260/OD280 value was measured with an ultraviolet spectrophotometer to evaluate the purity and concentration of RNA. Total RNA was reverse-transcribed into cDNA according to the following procedures: 25°C for 5 min; 42°C for 30 min, and 85°C for 5 min. RT-qPCR was utilized to examine target gene expression on the ABI 12K fluorescence RT-qPCR instrument (ABI, USA). GAPDH served as an internal reference. Homo TrxR1: 5'-CCCTGGTTGTTGGAGCAT-3' (forward), 5'-TCTGAGTCGGCCTGGTGT-3' (reverse); Homo GAPDH: 5'-TCAAGAAGGTGGTGAAGCAGG-3' (forward), 5'-TCAAAGGTGGAGGAGTGGGT-3' (reverse). The relative expression level was determined with the $2^{-\Delta\Delta\text{CT}}$ method.

Western Blot

After being lysed by RIPA lysis buffer (P0013B; Beyotime) on ice for 30 min, cells were centrifugated at 12 000 rpm for 10 min. The supernatant was harvested to another EP tube. The protein concentrations were assessed using a BCA kit (P0009; Beyotime). We added 5×SDS loading buffer according to the volume of the lysate, and samples were boiled at 100°C for 5 min. Specimens were separated via SDS-PAGE and transferred onto PVDF membranes. The PVDF membranes were washed with TBST and sealed with 5% milk/TBST at room temperature

for 1 h. After rinsing using TBST, primary antibodies against TrxR1 (1: 6000; 11117-1-AP; Proteintech, Chicago, USA), TXNIP (1: 1000; 18243-1-AP; Proteintech), p-ERK (1: 1000; #9101; CST, USA), p-AKT (1: 2000; #4060; CST), Bcl-2 (1: 1000; 12789-1-AP; Proteintech), Bax (1: 1000; WL01637; Wanleibio, Shenyang, China) and GAPDH (1: 5000; ATPA00013Rb, Atagenix, Wuhan) were diluted with 1% BSA/PBST as recommended, which were utilized for incubation of the membrane overnight at 4°C . Then, the PVDF membranes were incubated with horseradish peroxidase-labeled goat anti-rabbit (1: 5000; SA00001-2; Wuhan, Sanying, Wuhan, China) or anti-mouse secondary antibodies (1: 5000; SA00001-1; Sanying) diluted by 5% milk/PBST at room temperature for 1 h. After washing, the equal amounts of enhanced luminol reagent and oxidizing reagent were diluted by ddH_2O , and then added dropwise to the sealing film. The front side of the PVDF film was exposed to the luminescent reagent for 2 min. After the PVDF was turned over, the results were observed using the gel imaging system.

Apoptosis Assay

Apoptotic levels were assessed utilizing apoptosis detection kits (A211-02; Vazyme Biotech Co., Ltd, Nanjing, China). Cells were cultured in 6-well plates (6×10^5 cells). After the cells adhered to the wall, the corresponding drugs were added. After 48 h, the cells were centrifuged at 1000 rpm for 5 min. After removing the supernatant, $100 \mu\text{l}$ Annexin-V binding buffer was added to resuspend the cells. Then, samples were protected from light using $5 \mu\text{l}$ Annexin-V FITC and $5 \mu\text{l}$ PI for 15 min at room temperature. After adding $150 \mu\text{l}$ Annexin-V binding buffer, cell apoptosis was detected using a CytoFLEX S flow cytometer (Beckman, USA).

Cell cycle assay

Cells were seeded in 6-well plates (6×10^5 cells). Under treatment with different drugs for 48 h, 1 mL DNA staining solution was prepared, containing $20 \mu\text{l}$ PI solution (421301; Biolegend, California, USA), $1 \mu\text{l}$ Triton X-100 (T9284; sigma, USA), $0.2 \mu\text{l}$ Rnase A solution (B500474; Sangon Biotech), and PBS (C10010500BT; Life). After the cells were centrifuged at 1000 rpm for 5 min, the cells were resuspended in $100 \mu\text{l}$ PBS. The cells were fixed with 1 mL 70% ethanol at 4°C overnight. After centrifugation, cells were incubated with $300 \mu\text{l}$ DNA staining solution at room temperature away from light for 15 min. Cell cycle proportions were detected using CytoFLEX S flow cytometry (Beckman, USA).

Wound healing assay

A marker pen was used to draw a horizontal line on the back of the 6-well plate before inoculating cells on the culture plate. Using a $10\text{-}\mu\text{l}$ pipette tip, cell scratches perpendicular to the

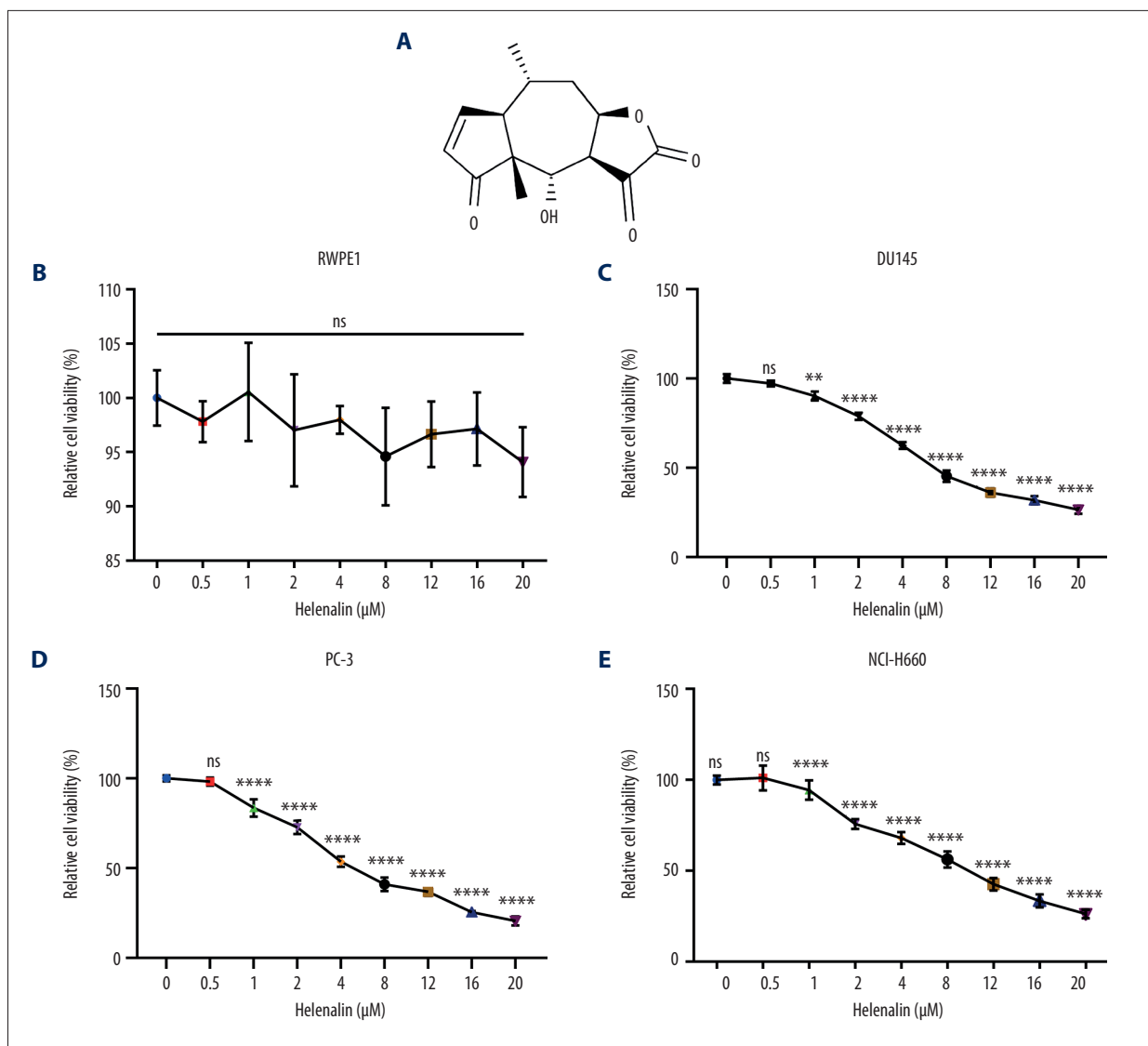


Figure 1. Helenalin represses the viability of human prostate cancer cells in a concentration-dependent manner. **(A)** Chemical structure of helenalin. **(B-E)** The effect of different doses of helenalin on the cellular viability for **(B)** human prostate RWPE1 cells, human AR-negative prostate cancer, **(C)** DU145, and **(D)** PC-3 cells, and **(E)** human neuroendocrine prostate cancer NCI-H660 cells. Ns – no statistical significance; ** $P < 0.01$; **** $P < 0.0001$.

well plate were made. The cell culture fluid was aspirated and the well plate was washed with PBS 3 times to wash away the cell debris generated by the scratch. Then, the serum-free medium was added. The culture plate was put into the incubator. After 0 h, 24 h, and 48 h, wound distance was assessed.

Transwell Assay

Matrigel was diluted 5 times with serum-free medium. We added 50 μL of Matrigel (356234; BD Biocoat, USA) to each transwell chamber and placed them in a 37°C incubator for 30 min. We ADDED 200 μL cell suspension (1.5×10^5 /ml) to the transwell chamber, AND 600 μL medium containing 10% FBS

was added to the lower chamber. After culturing at 37°C for 48 h, the culture solution in the well was discarded, and cells were washed twice with PBS. Then, cells were fixed with 4% PFA (P0099; Beyotime) for 10 min and stained with crystal violet (C0121; Beyotime) for 10 min. The upper chamber cells were wiped with a cotton swab. The migrated cells were investigated under a microscope.

Statistical Analysis

Data are presented as mean ± standard deviation. The statistical analyses were presented via GraphPad Prism 7 software (GraphPad Prism, USA). Comparisons with multiple groups

were performed via one-way analyses of variance, followed by Tukey's multiple comparisons tests. Differences with $P < 0.05$ were statistically significant.

Results

Helenalin represses the viability of human prostate cancer cells in a concentration-dependent manner

We first observed that helenalin (Figure 1A) at different concentrations did not affect the viability of human prostate RWPE1 cells (Figure 1B). Two kinds of AR-negative prostate cancer cells (DU145 and PC-3) were treated with different concentrations of helenalin. As shown in Figure 1C, as the concentration of helenalin increased, the survival rate of DU145 cells gradually and distinctly decreased; 8 μM was selected as the optimal concentration of helenalin for DU145 cells. Similarly, helenalin significantly suppressed the viability of PC-3 cells in a dose-dependent manner (Figure 1D); 4 μM was chosen as the final concentration of helenalin for PC-3 cells in further experiments. Also, we found that the viability of human neuroendocrine prostate cancer NCI-H660 cells was distinctly inhibited by helenalin (Figure 1E). Collectively, our data suggested that helenalin treatment inhibits prostate cancer cell viability in a concentration-dependent manner.

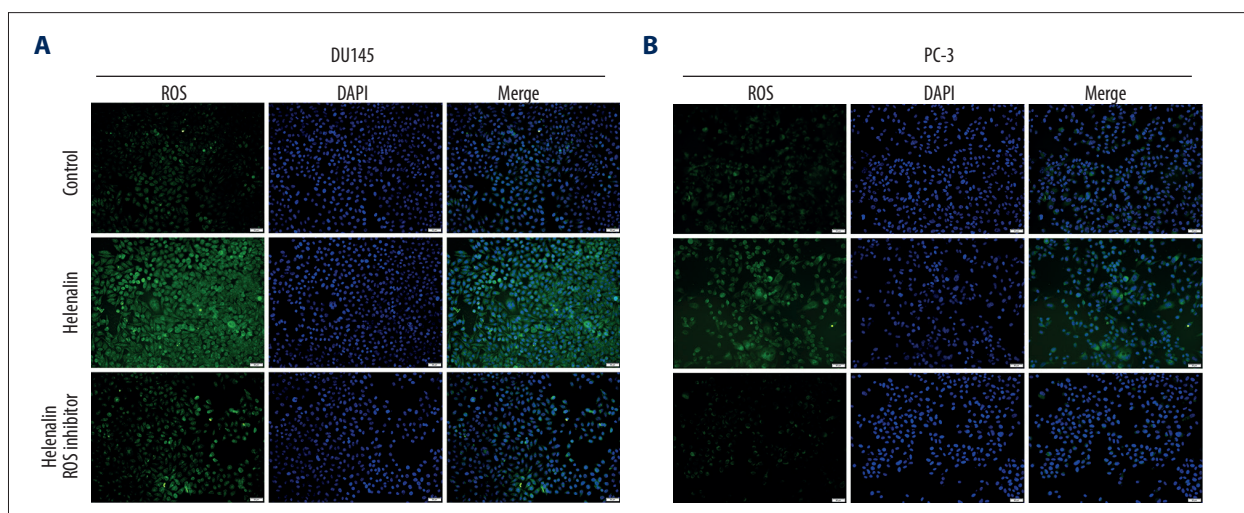
Helenalin induces ROS generation and suppresses TrxR1 expression by ROS in prostate cancer cells

We further analyzed whether helenalin could increase the level of ROS in prostate cancer cells, thereby inducing cell death of cancer cells. DCFH-DA staining was performed to detect the generation of ROS in the 2 kinds of cells. Our results showed that exposure to helenalin increased ROS levels in DU145 (Figure 2A) and PC-3 cells (Figure 2B) under a fluorescence

microscope. However, pre-treatment with ROS inhibitor NAC for 1 h distinctly ameliorated the increase in ROS levels induced by helenalin. Furthermore, our data suggested that TrxR1 mRNA expression was distinctly decreased in DU145 (Figure 2C) and PC-3 cells (Figure 2D) after exposure to helenalin. Nevertheless, ROS inhibitor pre-treatment reversed this inhibitory effect on TrxR1 expression induced by helenalin. The similar results were found at the protein level. As shown in Figure 2E-2G, TrxR1 protein expression was significantly suppressed after treatment with helenalin in prostate cancer cells, which was ameliorated after pre-treatment with ROS inhibitor. We further investigated the functional changes in downstream effects by detecting changes of TXNIP and ERK expressions and AKT activity. The results showed that helenalin treatment distinctly lowered the expression of TXNIP (Figure 2H, 2I), p-ERK (Figure 2J, 2K), and p-AKT (Figure 2L, 2M) in DU145 and PC-3 cells (Figure 2N). The inhibitory effects of helenalin on TXNIP, p-ERK, and p-AKT expressions were ameliorated by ROS inhibitor pre-treatment. Thus, helenalin induced ROS generation and suppressed TrxR1 expression by ROS in prostate cancer cells.

Helenalin Induces ROS-mediated Apoptosis And Cell Cycle Arrest in Prostate Cancer Cells

It has been reported that ROS is involved in regulating apoptosis and cell cycle in prostate cancer cells [23]. Thus, our study further investigated whether helenalin could affect ROS-mediated apoptosis and cell cycle arrest in 2 prostate cancer cell lines via flow cytometry. First, our data suggested that helenalin exposure markedly promoted apoptosis of DU145 and PC-3 cells (Figure 3A-3D). However, under pre-treatment with ROS inhibitor, the pro-apoptotic effect of helenalin was distinctly weakened in the 2 cell lines (Figure 3A-3D). We also assessed the cell cycle. The results showed that treatment with helenalin prominently prolonged the G0/G1 phase but shortened the S phase in DU145 and PC-3 cells (Figure 3E-3H). Nevertheless, pre-treatment



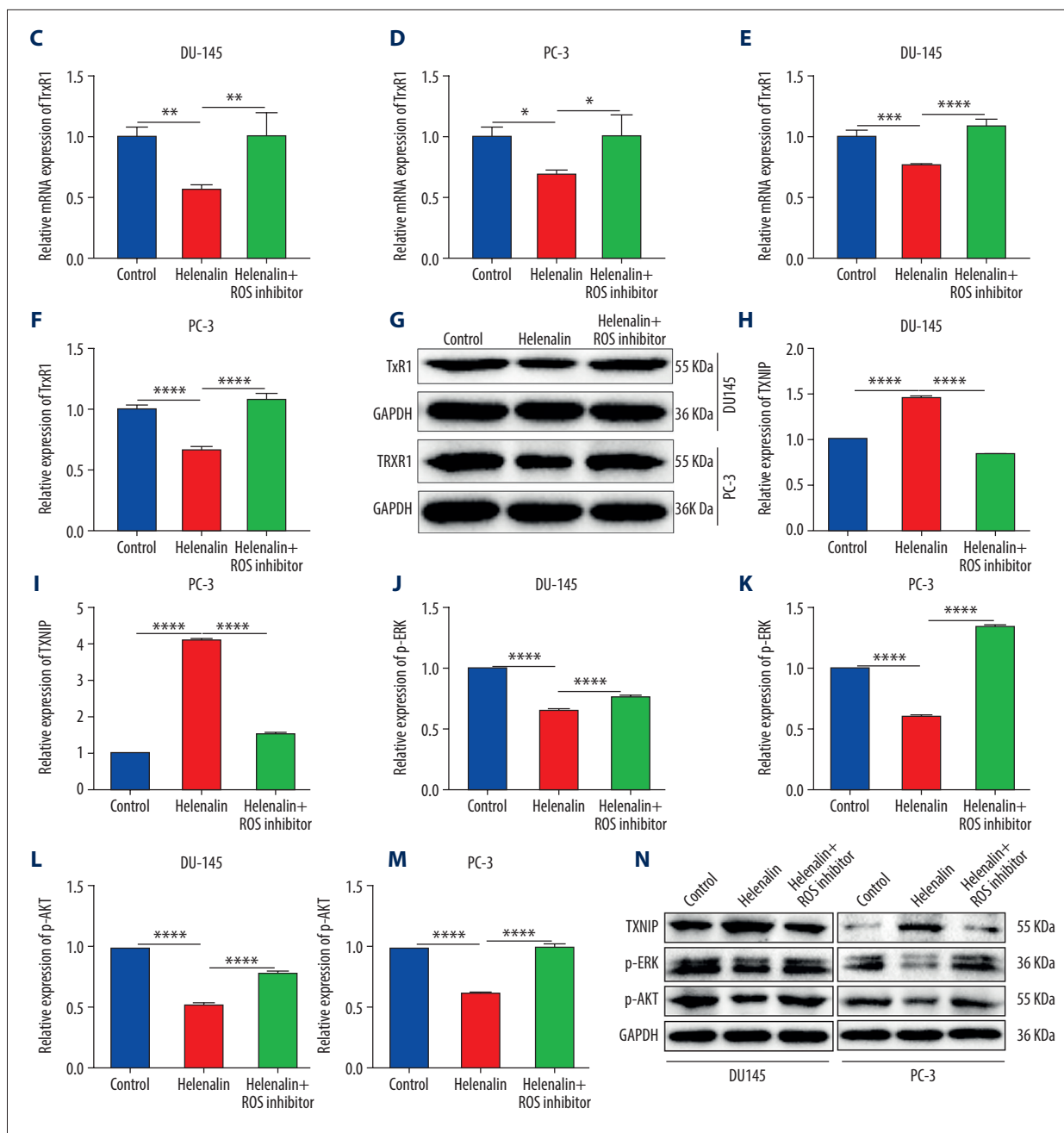
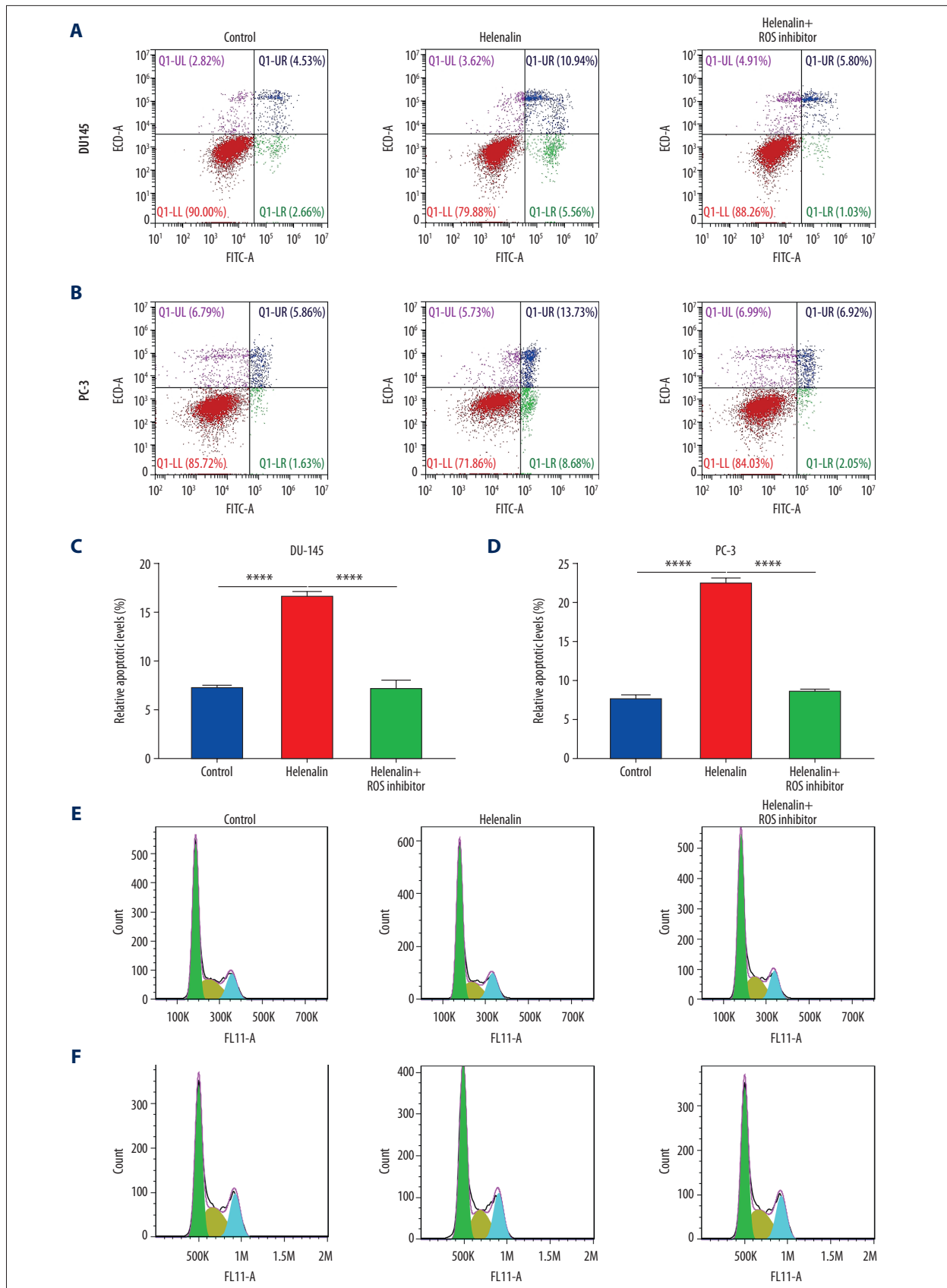


Figure 2. Helenalin induces reactive oxygen species and suppresses TrxR1 expression in prostate carcinoma cells. (A, B) The ROS levels were examined for 2 prostate carcinoma cell lines exposed to helenalin and/or ROS inhibitor by DCFH-DA staining. Bar=50 μ M. (C, D) RT-qPCR was carried out to examine the mRNA expression of TrxR1 in DU145 or PC-3 cells exposed to helenalin and/or ROS inhibitor. (E-G) Western blot analysis was performed to determine the expression of TrxR1 protein in the 2 cells after treatment with helenalin and/or ROS inhibitor. (H-N) Western blot was utilized for detection of the expression of TXNIP, p-ERK, and p-AKT in the 2 cell lines following treatment with helenalin and/or ROS inhibitor. * $P < 0.05$; ** $P < 0.01$; *** $P < 0.001$; **** $P < 0.0001$.



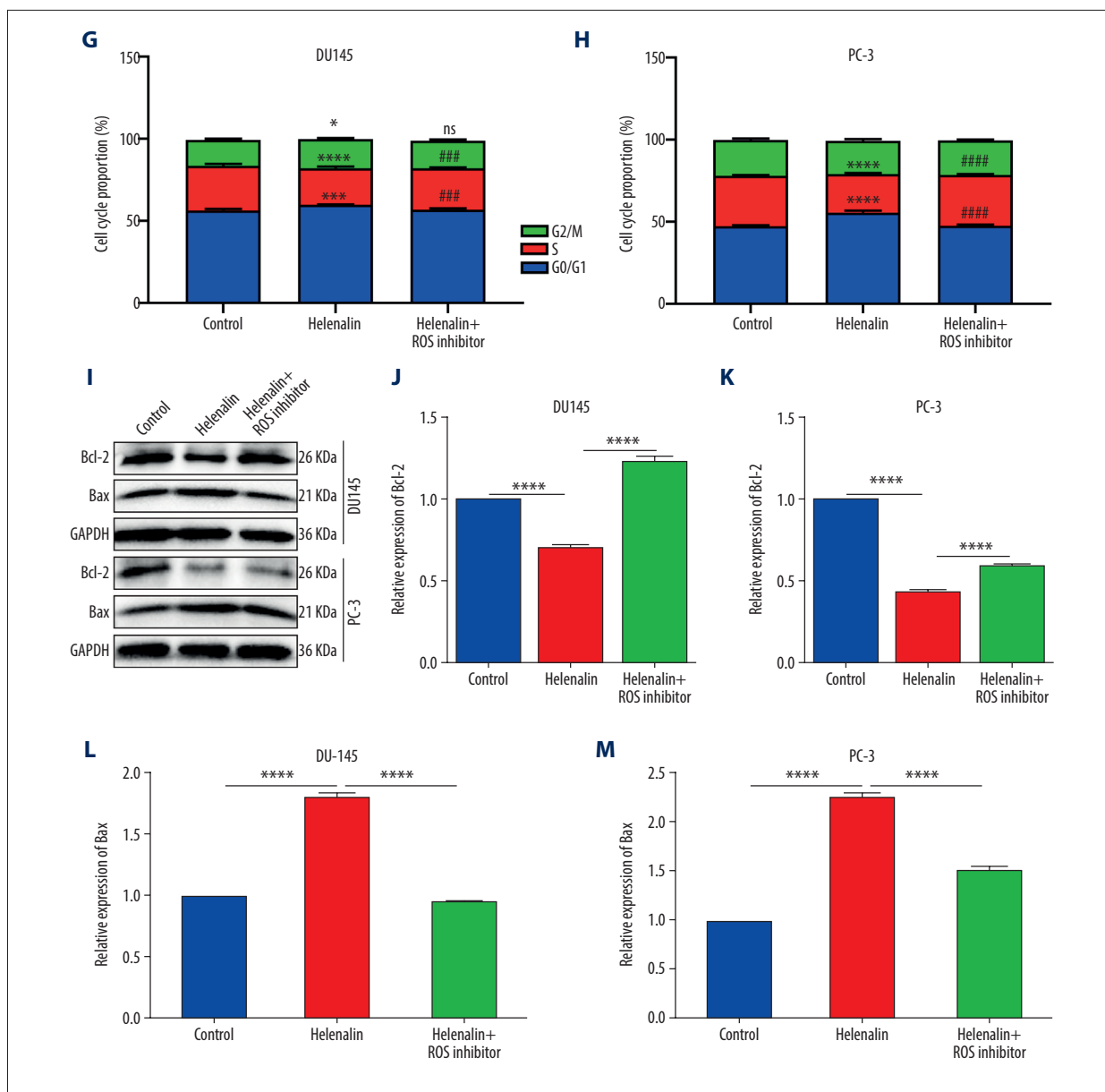


Figure 3. Helénalin induces ROS-mediated apoptosis as well as cell cycle arrest in prostate cancer cells. (A-D) Apoptotic levels were determined in DU145 and PC-3 cells treated with helénalin and/or ROS inhibitor. **** $P < 0.0001$. (E-H) Cell cycle was assessed in DU145 and PC-3 cells following treatment with helénalin and/or ROS inhibitor. (I-M) Western blot was carried out for examination of Bcl-2 and Bax expressions in DU145 and PC-3 cells following treatment with helénalin and/or ROS inhibitor. Compared to controls, * $P < 0.05$; ** $P < 0.001$, and **** $P < 0.0001$. Compared to helénalin group, ns: not significant; #### $P < 0.0001$.

with ROS inhibitor markedly reversed the effect of helénalin-induced cell cycle arrest (Figure 3E-3H). We also detected apoptosis markers Bcl-2 and Bax by western blot (Figure 3I), showing that helénalin treatment reduced Bcl-2 expression (Figure 3J, 3K) and elevated Bax expression (Figure 3L, 3M) in the 2 cell lines, which were ameliorated by ROS inhibitor pre-treatment. Taken together, our data demonstrated that helénalin induces ROS-mediated apoptosis and cell cycle arrest in prostate cancer cells.

Helénalin Significantly Suppresses TrxR1 Expression in Prostate Cancer Cells

We further assessed whether helénalin effectively inhibits the expression of TrxR1 in prostate cancer cells. To silence TrxR1 expression, 3 siRNAs against TrxR1 were transfected into DU145 and PC-3 cells. RT-qPCR results confirmed that TrxR1 expression was effectively silenced by the 3 siRNAs in the 2

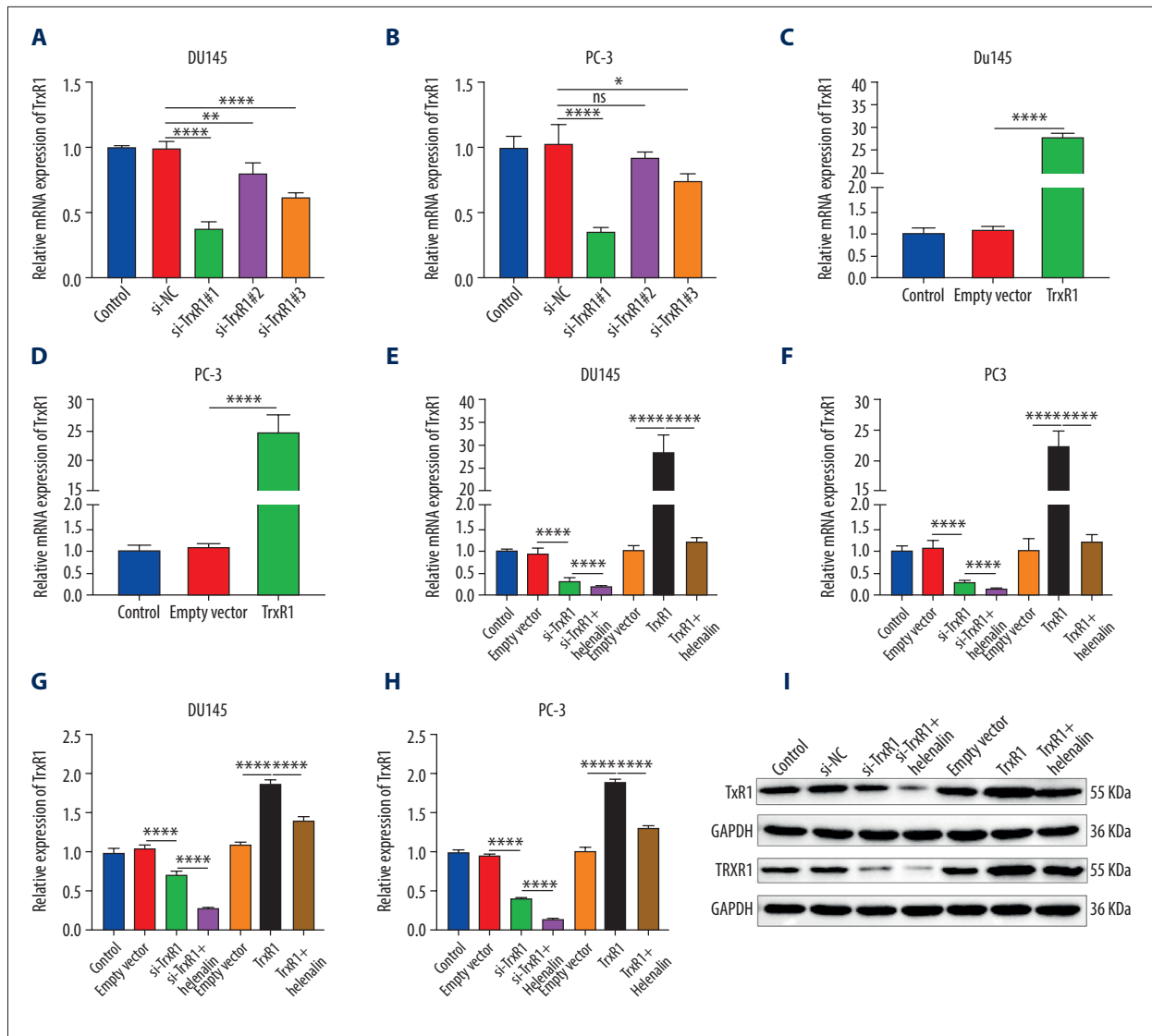


Figure 4. Helenalin treatment significantly suppresses TrxR1 expression in prostate carcinoma cells. (A, B) RT-qPCR was utilized to validate the knockdown effects of siRNAs against TrxR1 in 2 prostate carcinoma cell lines. (C, D) The overexpression effects of TrxR1 plasmid were verified in 2 prostate carcinoma cell lines by RT-qPCR. (E, F) RT-qPCR was performed to determine the mRNA expression of TrxR1 in 2 prostate carcinoma cells exposed to si-TrxR1, TrxR1 plasmid, and/or helenalin. (G-I) The protein expression of TrxR1 was assessed in the 2 cell lines treated with si-TrxR1, TrxR1 plasmid, and/or helenalin via western blot. ns: not significant; * $P < 0.05$; ** $P < 0.01$, and **** $P < 0.0001$.

cell lines (Figure 4A, 4B). Among them, si-TrxR1#1 exhibited the best knockout effect, which was used for further experiments. Furthermore, TrxR1 was distinctly overexpressed by transfection with TrxR1 plasmid in DU145 (Figure 4C) and PC-3 cells (Figure 4D), which was confirmed by our RT-qPCR. The inhibitory effect of helenalin on TrxR1 was further analyzed. As shown in Figure 4E and 4F, helenalin significantly exacerbated the decrease in TrxR1 mRNA expression induced by si-TrxR1. Moreover, the increase in TrxR1 mRNA expression induced by TrxR1 plasmid was ameliorated after co-treatment with helenalin (Figure 4E, 4F). Western blot results also showed that

helenalin exposure aggravated the reduction of TrxR1 protein expression for DU145 and PC-3 cells transfected with si-TrxR1 (Figure 4G-4I). Additionally, compared to transfection with TrxR1 plasmid, TrxR1 protein expression was distinctly decreased following co-treatment with helenalin (Figure 4G-4I). Collectively, our results show that helenalin treatment markedly lowered TrxR1 expression in prostate cancer cells.

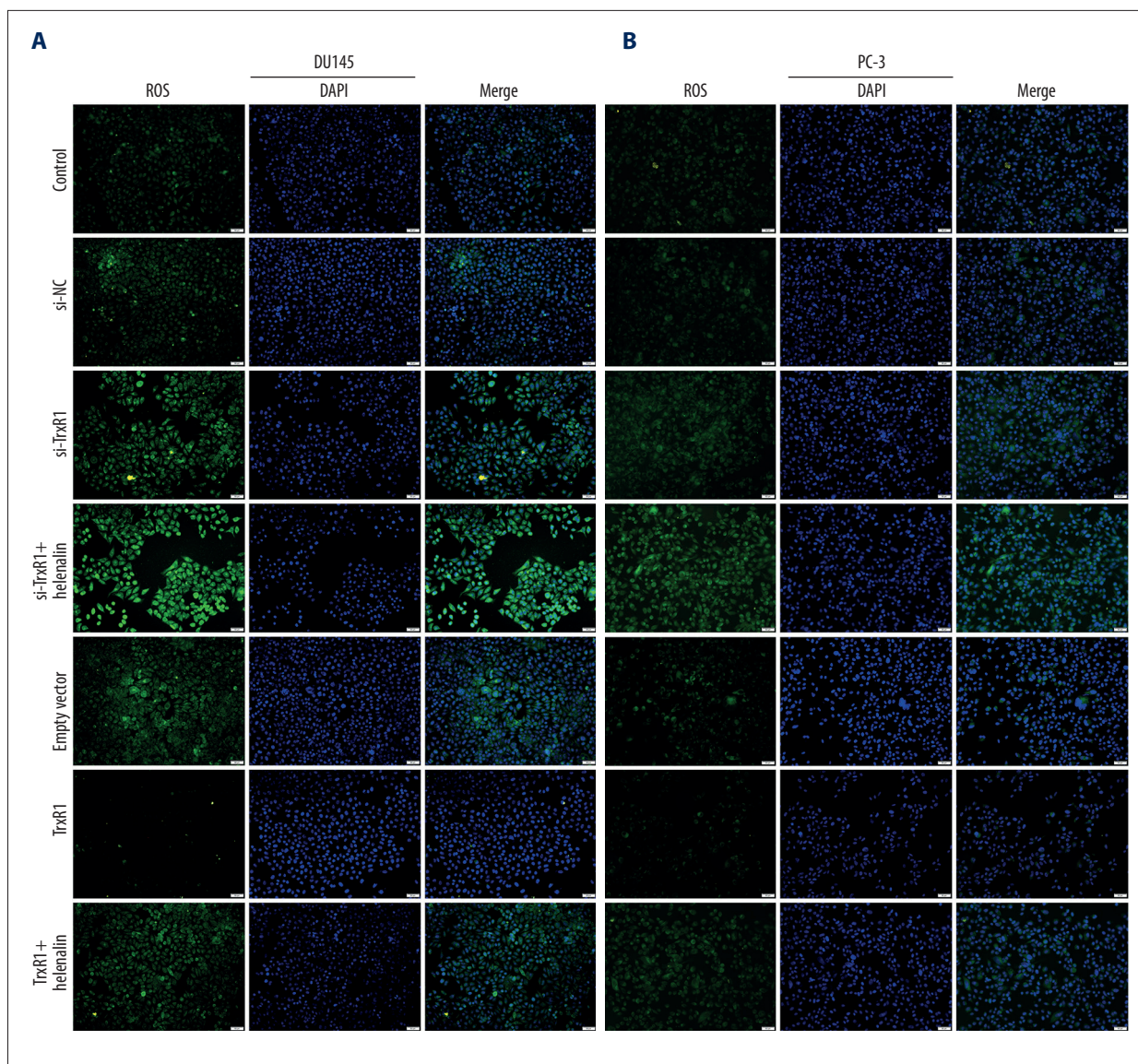


Figure 5. Helenalin exposure promotes ROS generation by suppression of TrxR1 in prostate carcinoma cells. **(A, B)** The ROS levels were examined for 2 prostate carcinoma cells exposed to si-TrxR1, TrxR1 plasmid, and/or helenalin by DCFH-DA staining. Bar=50 μ M.

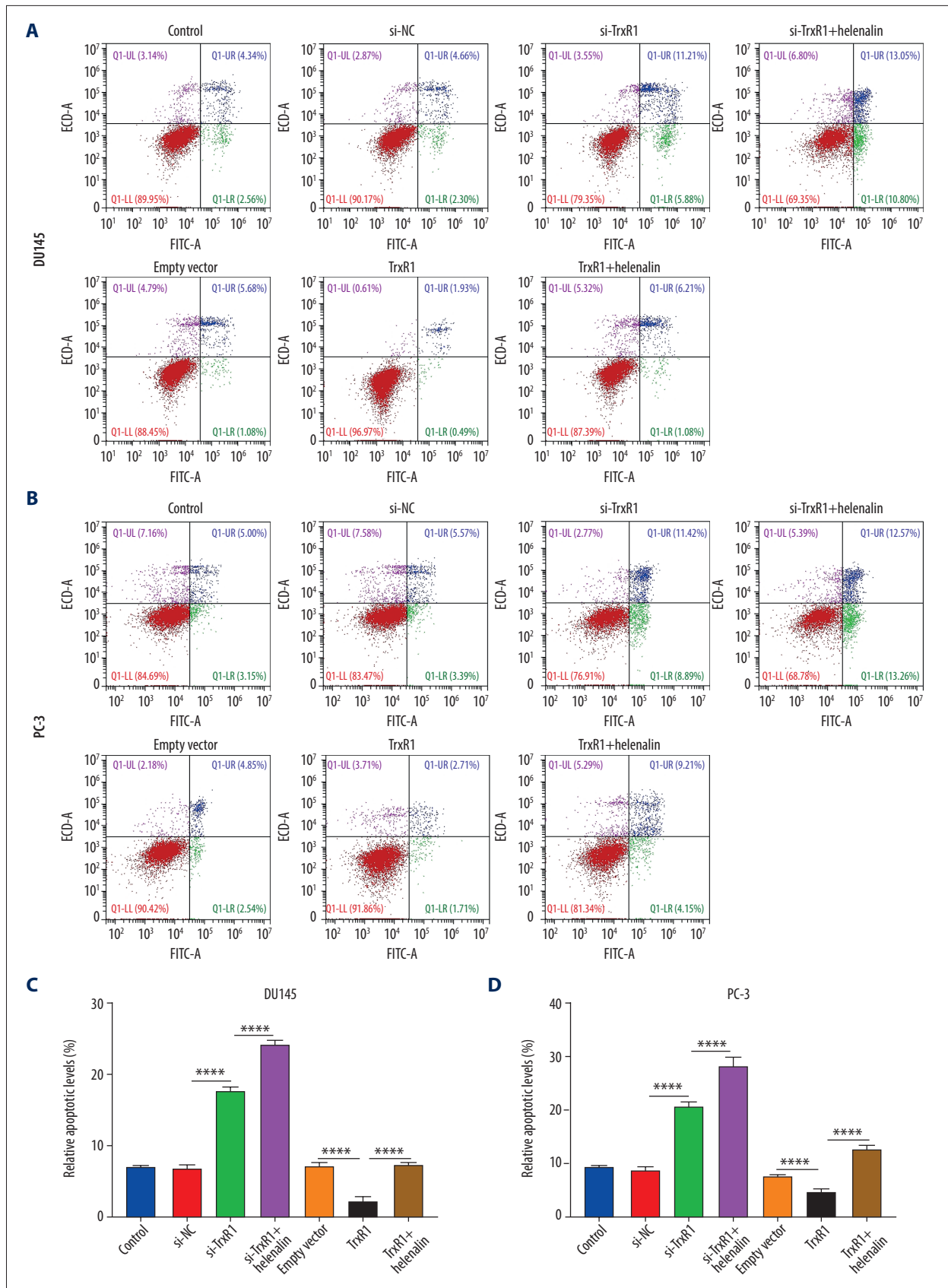
Helenalin Promotes ROS Generation by Suppression of TrxR1 in Prostate Cancer Cells

Whether helenalin can alter ROS production by targeting TrxR1 was explored in more depth. By DCFH-DA staining, we detected the production of ROS in prostate carcinoma cells. Compared to si-NC, ROS production was markedly elevated in the 2 cell lines following transfection with si-TrxR1 (**Figure 5A, 5B**). After co-treatment with helenalin and si-TrxR1, there were higher ROS levels in prostate carcinoma cells than in the si-TrxR1 group, suggesting that helenalin exposure could reinforce ROS production induced by TrxR1 knockdown (**Figure 5A, 5B**). Compared to the empty vector group, ROS levels were distinctly lowered

in the TrxR1 overexpression group. However, the increase in ROS levels was ameliorated after co-treatment with helenalin. Collectively, our findings revealed that helenalin treatment could facilitate ROS production via suppression of TrxR1 in prostate cancer cells.

Helenalin Treatment Induces Apoptosis and Cell Cycle Arrest via Targeting TrxR1 in Prostate Cancer Cells

Flow cytometry was performed to observe whether helenalin treatment could induce apoptotic levels and cell cycle arrest via inhibiting TrxR1 in 2 kinds of prostate cancer cells. As depicted in **Figure 6A-6D**, TrxR1 knockdown markedly elevated apoptotic



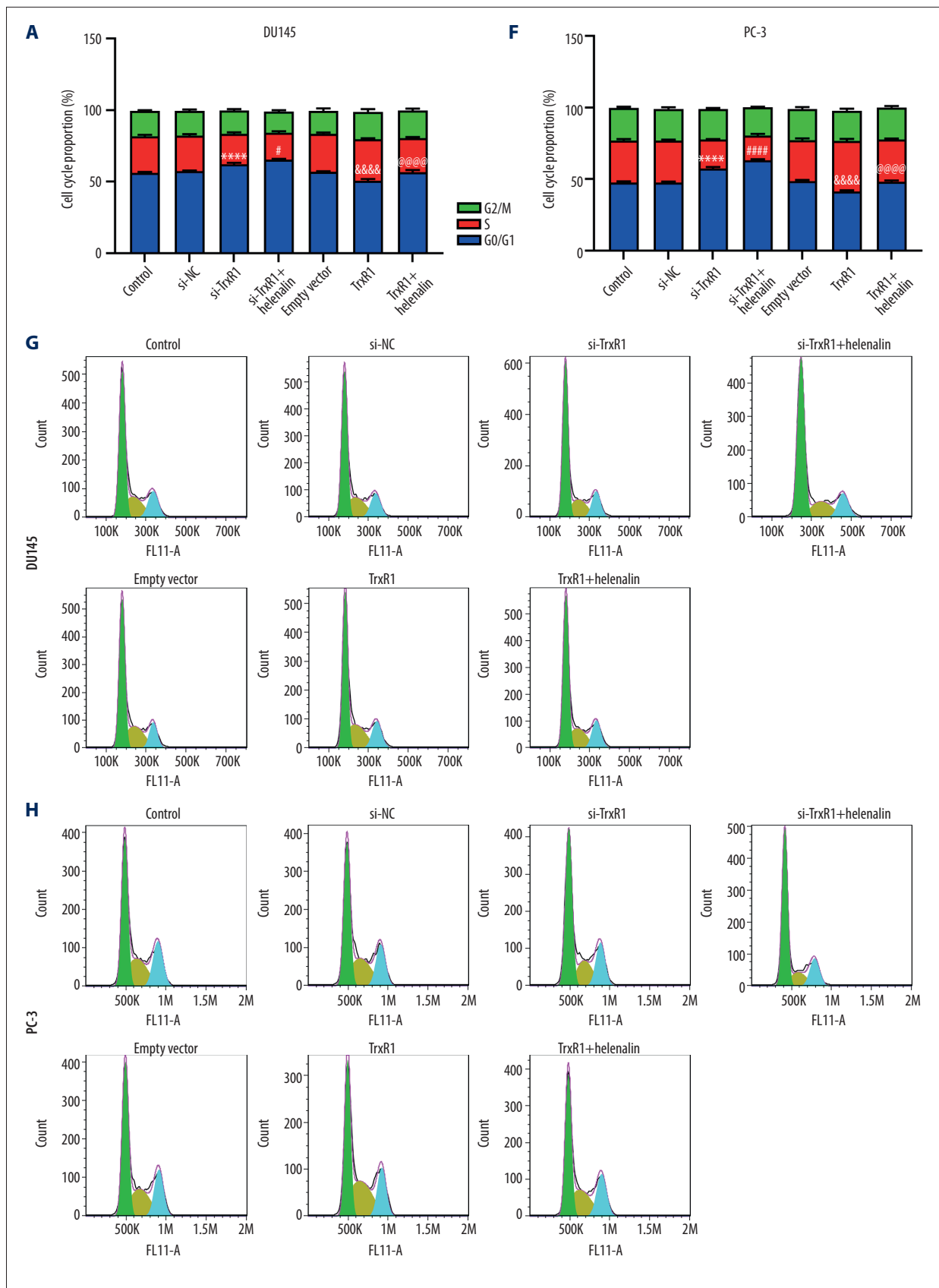
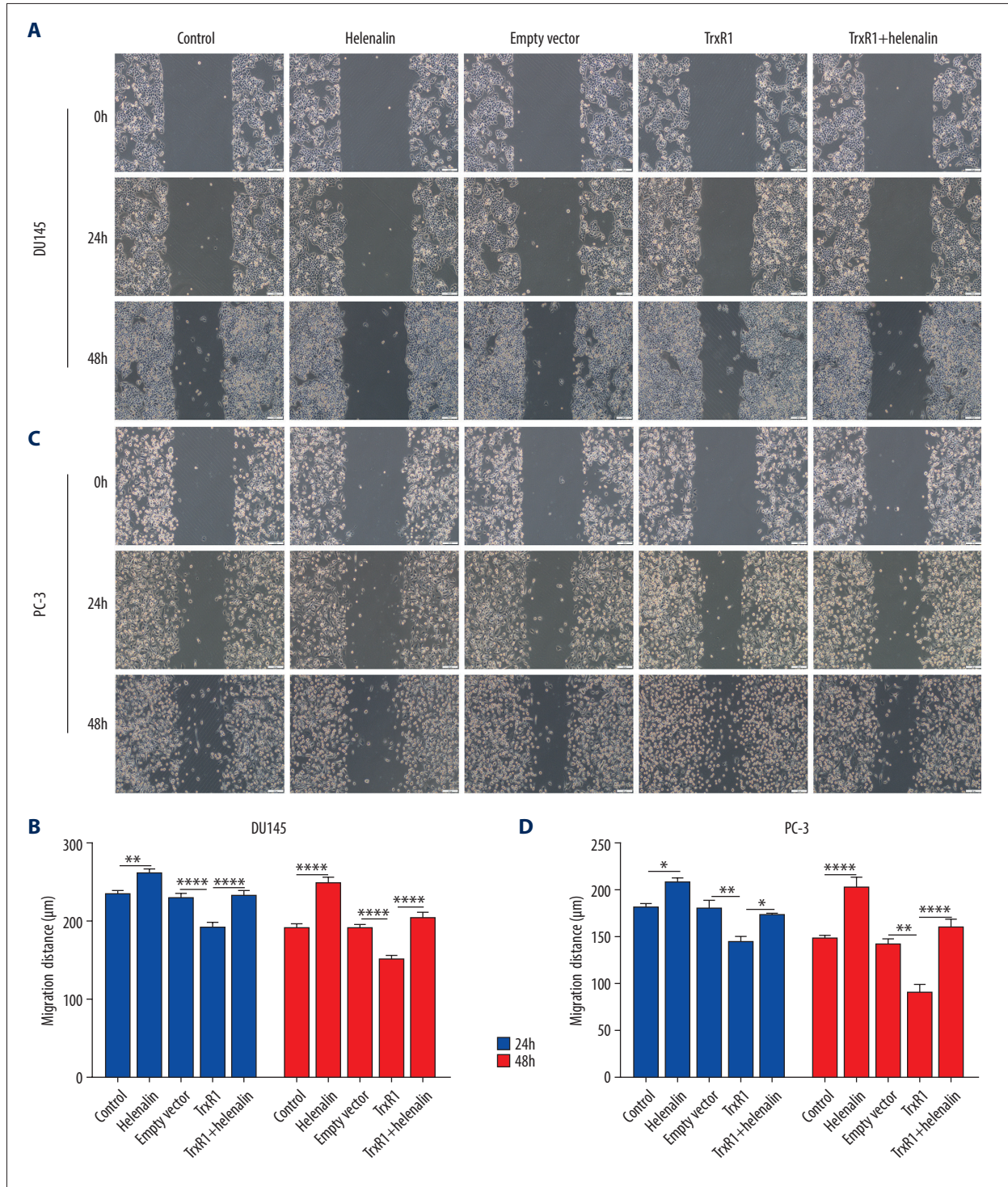


Figure 6. Helenalin treatment induces apoptosis and cell cycle arrest through suppressing TrxR1 expression for prostate carcinoma cells. **(A-D)** Apoptotic levels were examined in 2 prostate carcinoma cells exposed to si-TrxR1, TrxR1 plasmid and/or helenalin by flow cytometry. **** $P < 0.0001$. **(E-H)** Cell cycle was evaluated in the 2 prostate cancer cells following treatment with si-TrxR1, TrxR1 plasmid, and/or helenalin by flow cytometry. Compared to si-NC, **** $P < 0.0001$. Compared to si-TrxR1, # $P < 0.05$ and #### $P < 0.0001$. Compared to empty vector, &&&& $P < 0.0001$. Compared to TrxR1, @@@@ $P < 0.0001$.



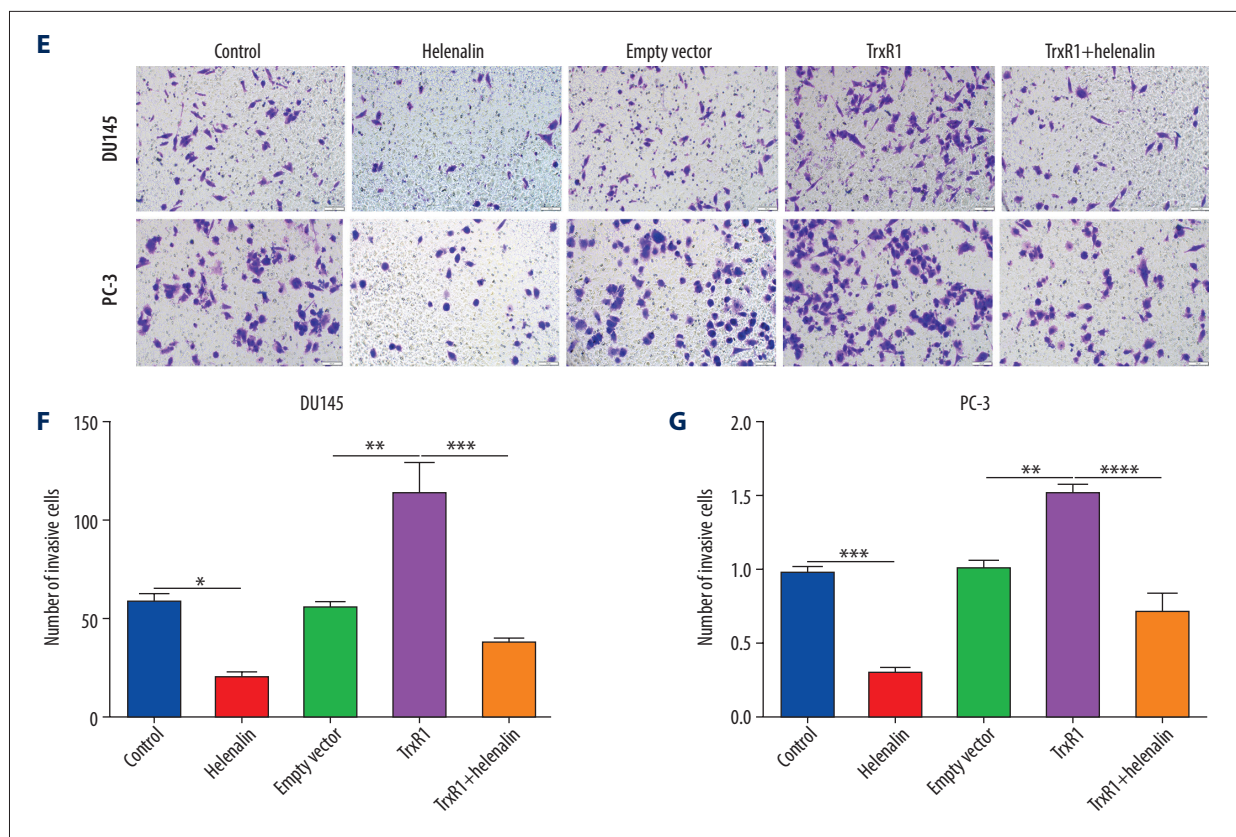


Figure 7. Helenalin suppresses migration and invasion by TrxR1 expression in prostate carcinoma cells. (A–D) Migration distance was detected in (A, B) DU145 and (C, D) PC-3 cells treated with TrxR1 plasmid and/or helenalin by wound healing assay. (E–G) The number of invasive DU145 and PC-3 cells was assessed following treatment with TrxR1 plasmid and/or helenalin by transwell assay. * $P < 0.05$; ** $P < 0.01$; *** $P < 0.001$; **** $P < 0.0001$.

levels, which was strengthened after co-treatment with helenalin in prostate carcinoma cells. The inhibitory effects of TrxR1 overexpression on apoptosis were investigated, showing amelioration by helenalin co-treatment. Furthermore, silencing TrxR1 markedly prolonged the G0/G1 phase, which was aggravated by co-treatment with helenalin (Figure 6E–6H). On the contrary, TrxR1 overexpression significantly shortened the G0/G1 phase. Nevertheless, the effect of shortening the G0/G1 phase was significantly improved by helenalin exposure (Figure 6E–6H). To sum up, our results demonstrated that helenalin induces apoptosis and cell cycle arrest via suppressing TrxR1 expression in prostate cancer cells.

Helenalin Treatment Restrains Migration and Invasion Through TrxR1 in Prostate Cancer Cells

The effects of helenalin on the migration and invasion of prostate cancer cells were further observed. Our results showed that the migrated ability of DU145 (Figure 7A, 7B) and PC-3 cells (Figure 7C, 7D) was distinctly suppressed after helenalin treatment. In contrast, TrxR1 overexpression significantly enhanced the migration ability of DU145 and PC-3 cells, which was ameliorated after helenalin co-treatment. Furthermore,

we found that helenalin treatment significantly reduced the number of invasive DU145 and PC-3 cells and the opposite results were achieved by TrxR1 overexpression (Figure 7E–7G). The stimulative effects of TrxR1 overexpression on invasion were weakened by helenalin co-treatment. Collectively, our results show that helenalin treatment can restrain migration and invasion through targeting TrxR1 in prostate cancer cells.

Discussion

There is an urgent need to find new candidate drugs for treating prostate cancer. Helenalin, a pseudoguaianolide natural product, exhibits effective anti-cancer effects in various human cancer cells [17,21,22]. However, it has not been completely determined whether helenalin can effectively promote the apoptosis of prostate cancer cells and its potential targets. In this study, we investigated the anti-cancer effects of helenalin in 2 prostate cancer cell lines. Helenalin treatment can promote ROS-mediated apoptosis and G0/G1 cell cycle arrest via targeting TrxR1 prostate cancer cells, indicating that helenalin could be a promising drug for prostate cancer.

Promotion of dysregulation of cell cycle progression and inhibition of cell proliferation have been considered as an effective strategy to limit the progression of cancers [24]. Our results showed that helenalin has a powerful pro-apoptosis effect on 2 types of prostate cancer cells by promoting cell cycle arrest in the G0/G1 phase. Intriguingly, we found that exposure to helenalin could induce ROS production in prostate cancer cells. As previous research showed, helenalin could alleviate the production of ROS in acute liver injury mice [18]. ROS is a mediator of cell death induced by helenin in solid tumor cells [25]. However, after pre-treatment with ROS inhibitor, the inhibitory effects of helenalin were alleviated in prostate cancer cells. Hence, one underlying mechanism to clarify the pro-apoptosis activity of helenalin could be through the ROS-dependent apoptosis and cell cycle arrest [26-28]. It has been reported that MHY440 could promote cell cycle arrest and apoptotic levels by ROS-dependent DNA injury in gastric carcinoma [29]. Brosimone I can induce G1 cell cycle arrest and elevate apoptotic levels in a ROS-mediated endoplasmic reticulum (ER) stress in colorectal carcinoma [30].

TrxR is a critical target molecule for developing anti-cancer agents [31]. TrxR1 has been determined to be involved in the pathogenesis of prostate cancer. Its upregulation is greater in PC-3 cells than in normal cells [32]. Targeting TrxR1 can delay castration recurrence in androgen-independent prostate cancer [33]. Our data showed that helenalin lowered the expression of TrxR1 in DU145 and PC-3 cells. After transfection with TrxR1 plasmid, helenalin reversed the overexpression of TrxR1 in prostate cancer cells. Thus, TrxR1 could be an underlying target of helenalin. Previously, suppressing TrxR1 was shown to induce the accumulation of ROS in gastric cancer cells [34],

and similar results were found in prostate carcinoma cells after knockdown of TrxR1. Also, overexpression of TrxR1 lowered the production of ROS. Silencing TrxR1 markedly accelerated apoptosis and G0/G1 cell cycle arrest of prostate cancer cells. The opposite results were detected when overexpressing TrxR1. It has been reported that suppression of TrxR1 could motivate ER stress-dependent apoptosis in breast cancer [35] and hepatocellular carcinoma [36] cell lines. Exposure to helenalin could reverse the inhibitory effects of TrxR1 overexpression on apoptosis as well as cell cycle arrest in DU145 and PC-3 cells, suggesting that helenalin could elevate apoptotic levels and induce G0/G1 cell cycle arrest through lowering TrxR1 expression in prostate cancer cells.

Taken together, our study shows a mechanism by which helenalin induces the anti-prostate cancer effect by targeting TrxR1, which was attributed to ROS-mediated cell apoptosis and cell cycle arrest in G1/G0 phase. Animal experiments are needed to determine whether helenalin could become a candidate drug for prostate cancer therapy.

Conclusions

Collectively, this study demonstrated that helenalin exerts an anti-prostate cancer effect by activation of ROS-mediated apoptosis and cell cycle arrest through inhibition of TrxR1. Hence, helenalin could be a promising anti-prostate cancer drug.

Conflict of Interest

None.

References:

1. Criscuolo D, Morra F, Giannella R, et al. Identification of novel biomarkers of homologous recombination defect in DNA repair to predict sensitivity of prostate cancer cells to PARP-inhibitors. *Int J Mol Sci.* 2019;20:3100
2. Xu R, Hu J. The role of JNK in prostate cancer progression and therapeutic strategies. *Biomed Pharmacother.* 2020;121:109679
3. Rice MA, Malhotra SV, Stoyanova T. Second-generation antiandrogens: From discovery to standard of care in castration resistant prostate cancer. *Front Oncol.* 2019;9:801
4. Hoffman KE, Penson DF, Zhao Z, et al. Patient-reported outcomes through 5 years for active surveillance, surgery, brachytherapy, or external beam radiation with or without androgen deprivation therapy for localized prostate cancer. *JAMA.* 2020;323:149-63
5. Habrowska-Górczyńska DE, Kowalska K, Urbanek KA, et al. Deoxyvalenol modulates the viability, ROS production and apoptosis in prostate cancer cells. *Toxins (Basel).* 2019;11:265
6. Yan Y, Chang L, Tian H, et al. 1-Pyrroline-5-carboxylate released by prostate Cancer cell inhibit T cell proliferation and function by targeting SHP1/cytochrome c oxidoreductase/ROS Axis. *J Immunother Cancer.* 2018;6:148
7. Cho HD, Lee JH, Moon KD, et al. Auriculasin-induced ROS causes prostate cancer cell death via induction of apoptosis. *Food Chem Toxicol.* 2018;111:660-69
8. Wang D, Gao Z, Zhang X. Resveratrol induces apoptosis in murine prostate cancer cells via hypoxia-inducible factor 1-alpha (HIF-1α)/reactive oxygen species (ROS)/P53 signaling. *Med Sci Monit.* 2018;24:8970-76
9. Wang Y, Zhang Y, Ru Z, et al. A ROS-responsive polymeric prodrug nano-system with self-amplified drug release for PSMA (-) prostate cancer specific therapy. *J Nanobiotechnology.* 2019;17:91
10. Ryu S, Lim W, Bazer FW, Song G. Chrysin induces death of prostate cancer cells by inducing ROS and ER stress. *J Cell Physiol.* 2017;232:3786-97
11. Ren X, Zou L, Lu J, Holmgren A. Selenocysteine in mammalian thioredoxin reductase and application of ebselen as a therapeutic. *Free Radic Biol Med.* 2018;127:238-47
12. Rodriguez-Garcia A, Hevia D, Mayo JC, et al. Thioredoxin 1 modulates apoptosis induced by bioactive compounds in prostate cancer cells. *Redox Biol.* 2017;12:634-47
13. Samaranyake GJ, Troccoli CI, Huynh M, et al. Thioredoxin-1 protects against androgen receptor-induced redox vulnerability in castration-resistant prostate cancer. *Nat Commun.* 2017;8:1204
14. Shan W, Zhong W, Zhao R, Oberley TD. Thioredoxin 1 as a subcellular biomarker of redox imbalance in human prostate cancer progression. *Free Radic Biol Med.* 2010;49:2078-87
15. Li K, Zheng Q, Chen X, et al. Isobavachalcone induces ROS-mediated apoptosis via targeting thioredoxin reductase 1 in human prostate cancer PC-3 cells. *Oxid Med Cell Longev.* 2018;2018:1915828
16. Cattaruzza L, Fregona D, Mongiat M, et al. Antitumor activity of gold(III)-dithiocarbamate derivatives on prostate cancer cells and xenografts. *Int J Cancer.* 2011;128:206-15
17. Jakobs A, Steinmann S, Henrich SM, et al. Helenalin acetate, a natural sesquiterpene lactone with anti-inflammatory and anti-cancer activity, disrupts the cooperation of CCAAT box/enhancer-binding protein β (C/EBPβ) and co-activator p300. *J Biol Chem.* 2016;291:26098-108
18. Li Y, Zeng Y, Huang Q, et al. Helenalin from *Centipeda minima* ameliorates acute hepatic injury by protecting mitochondria function, activating Nrf2 pathway and inhibiting NF-κB activation. *Biomed Pharmacother.* 2019;119:109435
19. Kriplani P, Guarve K. Recent patents on anti-cancer potential of helenalin. *Recent Pat Anticancer Drug Discov.* 2020;15:132-42
20. Huang PR, Yeh YM, Wang TC. Potent inhibition of human telomerase by helenalin. *Cancer Lett.* 2005;227:169-74
21. Liu J, Zhao Y, Shi Z, Bai Y. Antitumor effects of helenalin in doxorubicin-resistant leukemia cells are mediated via mitochondrial mediated apoptosis, loss of mitochondrial membrane potential, inhibition of cell migration and invasion and downregulation of PI3-kinase/AKT/m-TOR signalling pathway. *J Buon.* 2019;24:2068-74
22. Widen JC, Kempema AM, Villalta PW, Harki DA. Targeting NF-κB p65 with a Helenalin Inspired Bis-electrophile. *ACS Chem Biol.* 2017;12:102-13
23. Guo YX, Lin ZM, Wang MJ, et al. Jungermannone A and B induce ROS- and cell cycle-dependent apoptosis in prostate cancer cells *in vitro*. *Acta Pharmacol Sin.* 2016;37:814-24
24. O'Leary B, Finn RS, Turner NC. Treating cancer with selective CDK4/6 inhibitors. *Nat Rev Clin Oncol.* 2016;13:417-30
25. Hoffmann R, von Schwarzenberg K, López-Antón N, et al. Helenalin bypasses Bcl-2-mediated cell death resistance by inhibiting NF-κB and promoting reactive oxygen species generation. *Biochem Pharmacol.* 2011;82:453-63
26. Choi YH. Isorhamnetin induces ROS-dependent cycle arrest at G2/M phase and apoptosis in human hepatocarcinoma Hep3B cells. *Gen Physiol Biophys.* 2019;38:473-84
27. Hong SH, Cha HJ, Hwang-Bo H, et al. Anti-proliferative and pro-apoptotic effects of Licochalcone A through ROS-mediated cell cycle arrest and apoptosis in human bladder cancer cells. *Int J Mol Sci.* 2019;20:3820
28. Park C, Cha HJ, Lee H, et al. Induction of G2/M cell cycle arrest and apoptosis by genistein in human bladder cancer T24 cells through inhibition of the ROS-dependent PI3k/Akt signal transduction pathway. *Antioxidants (Basel).* 2019;8:327
29. Jang JY, Kang YJ, Sung B, et al. MHY440, a novel topoisomerase inhibitor, induces cell cycle arrest and apoptosis via a ROS-dependent DNA damage signaling pathway in AGS human gastric cancer cells. *Molecules.* 2018;24:96
30. Zhao Y, Zhou Y, Wang M. Brosimone I, an isoprenoid-substituted flavonoid, induces cell cycle G(1) phase arrest and apoptosis through ROS-dependent endoplasmic reticulum stress in HCT116 human colon cancer cells. *Food Funct.* 2019;10:2729-38
31. Arnér ES. Selenoproteins-What unique properties can arise with selenocysteine in place of cysteine? *Exp Cell Res.* 2010;316:1296-303
32. Hendrickx W, Decock J, Mulholland F et al. Selenium biomarkers in prostate cancer cell lines and influence of selenium on invasive potential of PC3 Cells. *Front Oncol.* 2013;3:239
33. Singh SS, Li Y, Ford OH, et al. Thioredoxin reductase 1 expression and castration-recurrent growth of prostate cancer. *Transl Oncol.* 2008;1:153-57
34. Zhang P, Shi L, Zhang T, et al. Piperlongumine potentiates the antitumor efficacy of oxaliplatin through ROS induction in gastric cancer cells. *Cell Oncol (Dordr).* 2019;42:847-60
35. Yin C, Dai X, Huang X, et al. Alantolactone promotes ER stress-mediated apoptosis by inhibition of TrxR1 in triple-negative breast cancer cell lines and in a mouse model. *J Cell Mol Med.* 2019;23:2194-206
36. Zhang Q, Chen W, Lv X, et al. Piperlongumine, a novel TrxR1 inhibitor, induces apoptosis in hepatocellular carcinoma cells by ROS-mediated ER stress. *Front Pharmacol.* 2019;10:1180